Journal of Himalayan Earth Sciences Volume, No., 2026 pp. 1-21

Application of Structural Analysis and Post-Stack Seismic Inversion for Reservoir Characterization in Kadanwari-Latif Block, Lower Indus Basin, Pakistan

Urooj Shakir[1,2], Muhammad Raiees Amjad[1,2*], Muyyassar Hussain[3], and Muhammad Haris Siddiqui[1]

[1] Department of Earth and Environmental Sciences, Bahria School of Engineering and Applied Sciences, Bahria University, Islamabad, 44000, Pakistan
[2] Centre of Research Excellence: Earth, Climate and Environment, Bahria University, Islamabad, 44000, Pakistan
[3] LMK Resources, Pvt. Ltd., Blue Area, Islamabad, Pakistan
**Corresponding Author: mraiees.buic@bahria.edu.pk*

Submitted Date:15/08/2026, Acceptance Date: 20/10/2026, Publication Date:---------

Abstract

Reservoir characterization provides detailed insight into the subsurface, particularly for hydrocarbon assessment. Seismic interpretation, along with an integrated data set, facilitates the interpretation, mapping, and quantification of potential reservoir zones. The basic aim of this research is to delineate good porosity-bearing intervals and the hydrocarbon potential of these zones. The sand intervals of the Lower Goru Formation are considered a challenging reservoir due to their heterogeneity in terms of lithology and, specifically, porosity. Quantification of reservoir characteristics (i.e., porosity and P-impedance) is made possible by utilizing 3D seismic and well data of the Kadanwari block. Structural geometries comprising horst and graben configurations associated with normal wrench-related faults were delineated through conventional seismic interpretation, and potential at the targeted reservoir, i.e., the B-interval of the Lower Goru Formation, has been estimated via petrophysical analysis. Furthermore, low impedance at the B-interval, evaluated through post-stack model-based seismic inversion, improved confidence in choosing this interval as a potential reservoir. Petrophysics not only helped to generate a good petro-elastic relationship between well and elastic seismic properties in the reservoir zone but also worked as a validating agent for the inverted elastic properties. Finally, a most vital factor, i.e., porosity, towards reservoir characterization, is predicted through regression analysis. The predicted porosities within the B-Sand interval of the Lower Goru Formation range from 11% to 17% with a correlation coefficient R^2 of 87%. A best-fit, high correlation is achieved between predicted (inverted) and measured porosity, validating the inversion results. The technique applied in this research can be easily implemented in other areas having similar tectonics and geology.

***Keywords*:** Seismic interpretation; Petro-elastic attributes; Model-based seismic inversion; Inverted porosity.

1 Introduction

Assessment of hydrocarbon potential serves as a vital tool in defining the economic viability of any field. In a hydrocarbon-productive basin, gas reserve estimation depends on characterization of reservoir rock properties, which are essential for developing plans and risk investigation (Nanda, 2016). Reservoir characterization requires integrated analysis and understanding of available seismic and well data. Acoustic impedance variation in subsurface rocks produces reflected amplitude on seismic sections, which provides a distribution of different lithologies. In the evaluation of reservoir properties, band-limited contrast is used, and by applying deconvolution operations, it can be further improved (Rashid et al., 2022).

Seismic inversion, based on time travel, amplitude, and phase information contained in a seismogram, can be used to determine the elastic properties of rock utilizing seismic data. It presents a more accurate subsurface image. Acoustic impedance is considered the most crucial physical characteristic in seismic inversion analysis, which results from changes in subsurface density and velocity. P- and S-wave velocities, density, and other elastic parameters are determined using inverted impedance models, and these results are then used for fluid characterization (Bachrach, 2009). By further processing inverted seismic models, reservoir characteristics like shale/sand ratios and fluid saturation are estimated (Shakir et al., 2022; Babasafari et al., 2020; Hampson et al., 2000).

Seismic inversion analysis is classified into pre-stack and post-stack seismic inversion. AVO analysis, i.e., variation in seismic amplitudes with offset, can be applied to pre-stack data to estimate fluid and lithological properties. Seismic data showing amplitudes are converted into acoustic impedance (at zero offsets) in post-stack inversion using geological data, well logs, and seismic data (Amjad et al., 2023). At economical level final impedance models can be used to estimate reservoir characteristics (Ma, 2002; Mukerji et al., 2001). Seismic data is essential and used as input data to estimate rock physical properties. Seismic inversion usually requires seismic and well data along with a series of interpreted horizons as input data sets. As seismic data is a type of convolved and band-limited data set, removing the noise and decreasing any wavelet effects will have a strong impact on acoustic impedance, resulting in enhanced resolution of subsurface hydrocarbon-bearing zones (Ali et al., 2016; Hussain et al., 2023).

The research area is situated in the Lower Indus Basin, which is regarded as significant and one of the most prolific basins in terms of oil generation and production. This recent study evaluated the potential of Cretaceous-aged sands in the Kadanwari-Latif block. In the Lower Indus Basin, the Lower Goru Formation (LGF) is widely dispersed and serves as a significant target for hydrocarbons. Lower Goru Formation has heterogeneous thickness and reservoir characteristics despite its extensions (Sohail et al., 2020). The LGF's reservoir properties have changed because of contemporaneous depositional environments, variations in sea level during the Cretaceous period, shale intercalations, and distribution patterns (Craig et al., 2018; Umar et al., 2011). The study area and its surrounding hydrocarbon fields have proven the B-interval of the LGF to be the reservoir. It is made up of medium- to coarse-grained sandstone deposits in a shallow marine depositional environment, making it the most productive reservoir rock unit (Khalid et al., 2023).

To evaluate reservoir characteristics of the LGF, various studies were carried out previously on the basis of seismic structural/stratigraphical interpretations, petrophysical analysis, and rock physics modeling. This current study incorporates a 3D seismic cube along with wireline log data of the Kadanwari field to evaluate reservoir properties utilizing the post-stack inversion method. A 3D seismic cube is used for structural interpretation, and wireline log data from three wells (Kadanwari-01, 03, and 10) are used in petrophysical analysis. Well log data from the Kadanwari-01 well is used in inversion methods. In the initial step, a detailed seismic interpretation is carried out to delineate, mark, and map stratigraphic horizons and structural features in the subsurface (Fig. 7). Model-based inversion is carried out on the interpreted horizons/data to estimate rich zones in the B-Sand of LGF, Lower Indus Basin.

In this study, a regression-based porosity prediction approach was used to estimate reservoir property values. In this approach, impedance values obtained through inversion are used as an external attribute, while seismic and wireline log data are used as internal attributes (Ali et al., 2018). A regression-based porosity prediction, along with the combination of seismic inversion analysis, has been utilized for estimating porosity in the B-Sand of the

LGF; inverted impedance is used with a regression-based porosity prediction method.

2 Geological settings

Kadanwari Block is part of the Lower Indus Basin (LIB) (Fig. 1), bounded by the Jacobabad-Khairpur Horst to the east and northeast, the Mari-Kandhkot Horst to the west, and the Thar Platform to the south (Ali et al., 2022; Abubakar et al., 2026). The block's structural arrangements developed as a result of three main tectonic episodes. The first event involved erosion and uplift during the Late Cretaceous. The uplift axis is oriented NNE–SSW, but its degree is undefined. The second phase involved basement-embedded right-lateral wrench faults. These faults are generally oriented NNW–SSE, with a 'flower structure' generated by transtensional stresses.

The uplift/inversion in the Late Tertiary to the present in the Jacobabad High is the third major event, having a main impact on the study area by controlling the trapping mechanisms (Ahmad et al., 2007). There are appreciable thickness variations along with several positive structural geometries in the sedimentary layers responsible for hydrocarbon entrapment (Khan et al., 2023; Ahmad et al., 2004). Lower Indus Basin is further divided into the Central and Southern Indus Basin, demarcated by the Jacobabad-Khairpur High. Kadanwari area is located on the Jacobabad-Khairpur High's southeast flank (Ahmad and Ghazi, 2022). On the Precambrian basement of Jacobabad-Khairpur High, sedimentary cover can be up to 4000 m thick, and gas reserves are trapped in Eocene carbonates, Jurassic sandstones, and Cretaceous sandstones (Ali et al., 2022). A generalized stratigraphic column of LIB representing the petroleum play components is given in Figure 2.

The Ranikot Formation of the Paleocene, pinching out towards Jacobabad-Khairpur High, is evidence of the initial Paleogene uplift event disturbing Jacobabad-Khairpur High. By observing carbonate buildups and their associated deep-water marl deposits of the early Eocene and shales in the late Eocene, paleotopographers were able to determine the expansion of the subbasin and complex basin topography (Ghazij Shale). The basement-rooted faults are mostly oriented NNW-SSE (Ali et al., 2021), and shallow wrench faults cut through the entire strata of Cretaceous age, which ultimately terminate at the Cretaceous-Tertiary (K-T) level.

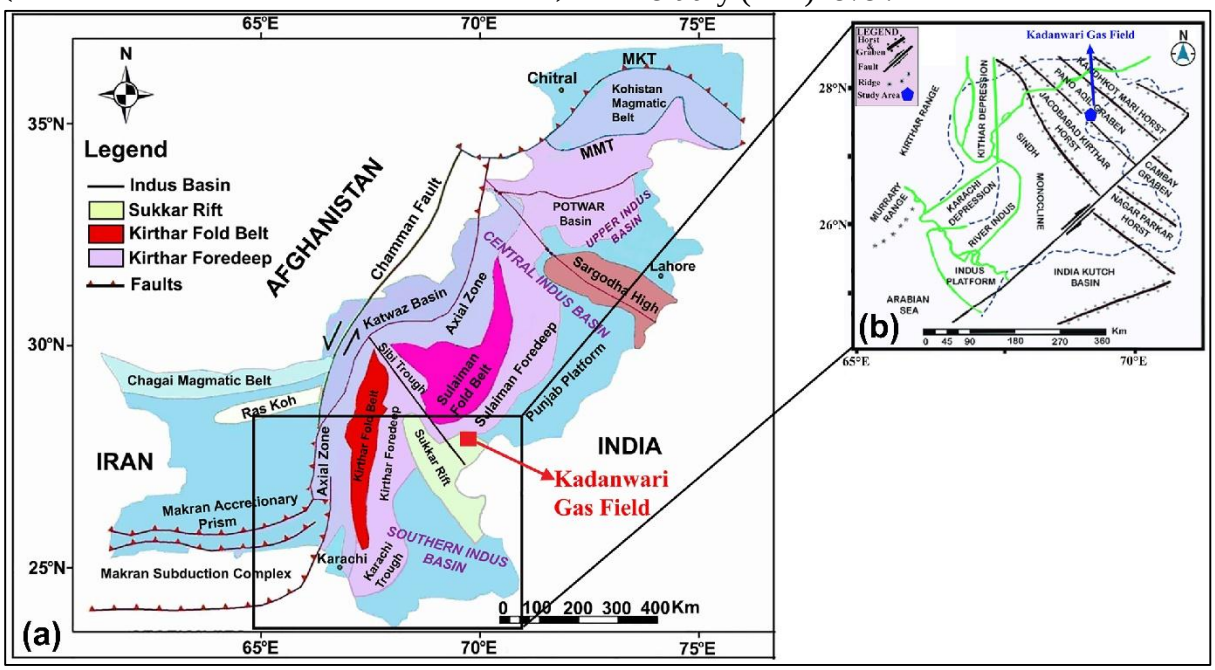

Fig. 1. (a). The map shows the Kadanwari gas field location with major geological features of LIB. (Khan et al., 2023). (b). Kadanwari block is located within the Pano-Aqil Graben, surrounded by the Mari-Kandhkot and Jacobabad Khairpur Horst (Ahmed et al., 2022).

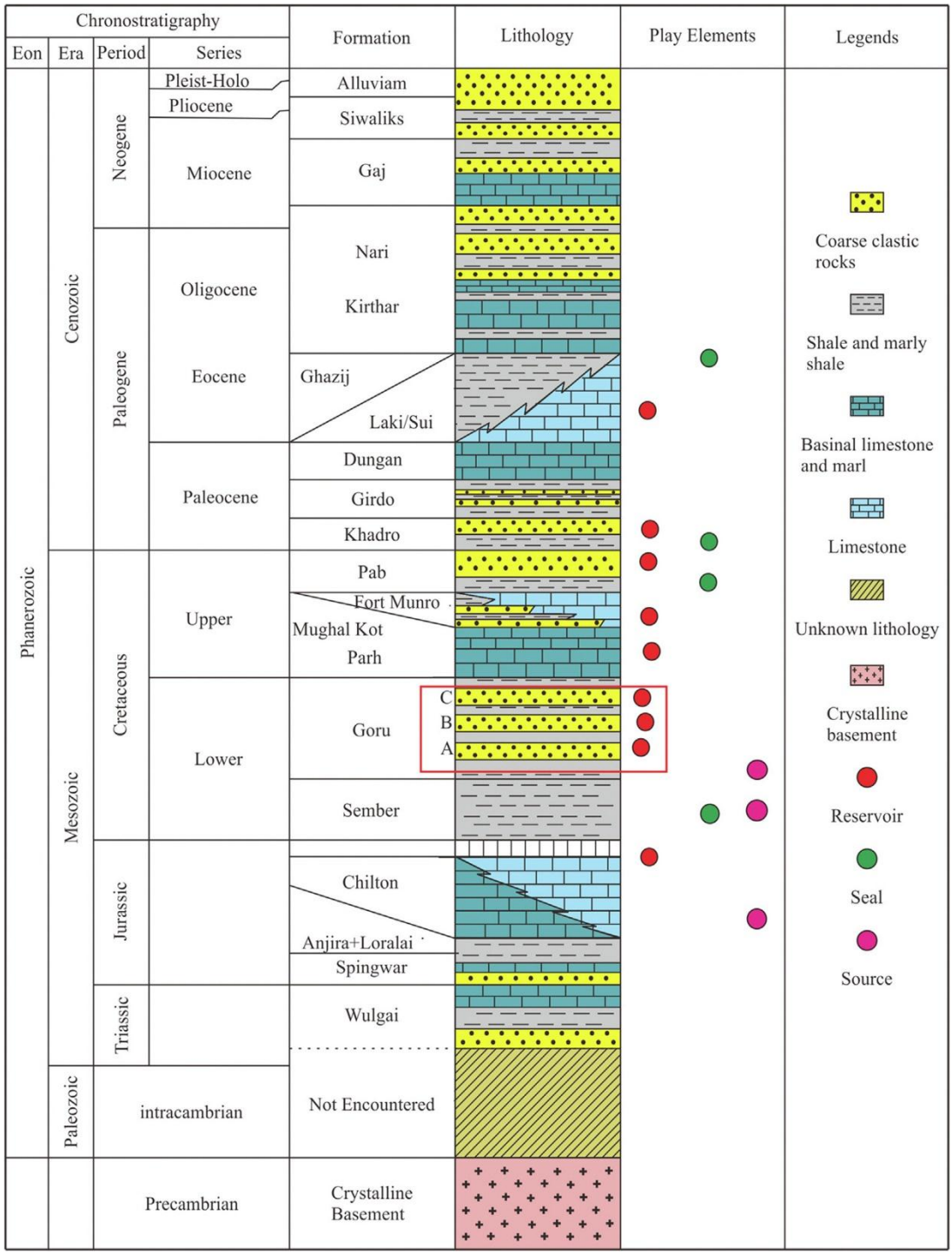

Fig. 2. Generalized stratigraphic column of the study area showing the major lithostratigraphic units from the crystalline basement to Recent deposits. Petroleum system elements of the region, showing the major source, reservoir, and seals, are also shown (Dar et al., 2023).

With the help of transtensional tectonics, the Indian and Eurasian plates collided, causing faulted geometry and the anticlockwise movement of the Indian plate (Ahmad et al., 2019). Peripheral forebulges were created because of crustal thrusting and nappe thrusting during the later events, i.e., lower Tertiary and Mesozoic, in paleo-highs, in the western and northwest regions of the region (Ahmad and Chaudhry, 2002). The Jurassic Chiltan limestone is overlain by the Cretaceous Sembar and LGF in terms of stratigraphy. Clastic sediments of the LGF are further categorized into members based on the sand-shale facies. The detailed nomenclature of the LGF is shown in Figure 3.

Lower Cretaceous Sembar Formation is regarded as a significant proven source in the basin, consisting primarily of shale but also containing sandstone, siltstone, and very thin layers of limestone. Sembar Formation, having type II/III kerogen, represents a potential source rock based on organic richness and thermal maturity. Medium to coarse sandstone that was deposited in a shallow marine environment can be found in the LGF. It is an economically productive reservoir in the study area as well as in the neighboring oil and gas fields (Khan and Khan, 2018). The primary cap rock in the Sembar-Goru petroleum system is made up of shales from the Upper Goru Formation. The thin shale layers within the LGF can serve as a potential seal for accumulation of hydrocarbons. Additionally, seal rocks include shale from the Tertiary-aged Ranikot Formation and Cretaceous-aged Sembar Formation (Naeem et al., 2016).

3 Dataset and Methodology

Integrated reservoir studies by utilizing geophysical and geological datasets are extremely useful in evaluating reservoir quality. The study focuses on evaluating the potential reservoir intervals by predicting vertical and lateral porosity variations. 3D post-stack seismic data cube of Kadanwari area has been utilized for delineating the subsurface structure and identification of prospects zones. The seismic cube comprises 140 inlines and 154 crosslines.

Both the shot-point and receiver intervals are 50 m, resulting in an acquired fold coverage of 50. The bin/CDP dimensions are 25 × 25 m, with an offset range of 50–4000 m. The seismic data have a dominant frequency of approximately 25 Hz. Petrophysical interpretation is used to identify the reservoir zones and non-reservoir zones in the subsurface using well log data. The petrophysical properties of the target reservoir interval have been evaluated through the wireline log data of Kadanwari-01, Kadanwari-03, and Kadanwari-10 wells. The log data include the gamma ray (GR) log, resistivity (LLD, LLS, MSFL) logs, density (RHOB) log, neutron porosity (NPHI) log, sonic (DT) log, and spontaneous potential (SP) log. The log curves have been used to compute the petrophysical properties of Lower Goru sand intervals.

NOMENCLATURE OF LOWER GORU FORMATION

	OGDCL			UTP		LASMO	OMV
Lower Goru	Upper Sands	"A" sands	Layer-1	Upper Sands	"A" sands	Shale out in north	Shale out
		Turk shale	Layer-2		Turk shale		
		"B" sands	Layer-3		"B" sands		
		Badin shale	Layer-4		Badin shale		
		"C" sands	Layer-5		"C" sands		
		Jhol shale			Jhol shale		
		"D" sands			"D" sands		
	Upper Shale			Upper Shale		"H" sand within U-shale	No significant sand body
	Middle Sand			Middle Sand		"G" sand	"D" sand interval
	Lower Shale/SABS (SABS: sands above basal sands)			Lower Shale		"F" sand within lower shale	"C" sand interval
	Basal Sand			Basal Sand		"E" sand	"B" sand interval
	Talhar Shale			Talhar Shale		"D" sand "C" sand within shale	
	Massive Sand			Lower Basal Sand		"B" sand	"A" sand interval
	Sembar			Sembar		"A" sand	Sembar

Modified after Nasar, 2000

Fig. 3. Nomenclature of LGF adopted by different exploration companies to demarcate the formation into several lithostratigraphic units (Ahmad and Ghazi, 2022).

Potential reservoir intervals are demarcated based on the trend of GR and resistivity logs along with neutron-density cross-over. These intervals are further evaluated for basic petrophysical properties including shale volumes, porosity, and fluid saturations. These potential sands are further categorized into pay and non-pay intervals by applying the petrophysical cut-offs for volume of shale (Vsh < 30%), porosity (PHIE > 5%), and water saturation (Sw < 50%). These empirically computed porosity curves are further utilized in seismic inversion and porosity prediction. The generalized methodological workflow utilized for the study is given in Figure 4, and the detailed workflow is discussed in the preceding subsections.

3.1 Seismic Interpretation

Seismic interpretation is the translation of seismic information into subsurface geological and structural features by using different techniques. Measurement of significant geology is done by seismic interpretation. Detail description of subsurface geology is not an easy task, so pitfall in interpretation may be ascertained. Seismic interpretation is important for finding hydrocarbons in oil and gas exploration. From different scientific investigations, interpretations are almost always non-unique (Dobrin and Savit, 1988). Seismic data interpretation is the process of finding evidence about the Earth's structures. It provides information about the area, discovers probable zones for investigative drilling wells, or guides exploration in previously revealed fields. Synthetic seismograms help to identify seismic reflectors and trace along the seismic line as shown in Figure 5 (Kearey et al., 2002). Evidence about prospect's potential and identification for best drilling locations is delivered by seismic interpretation (Tiab and Donaldson, 2015).

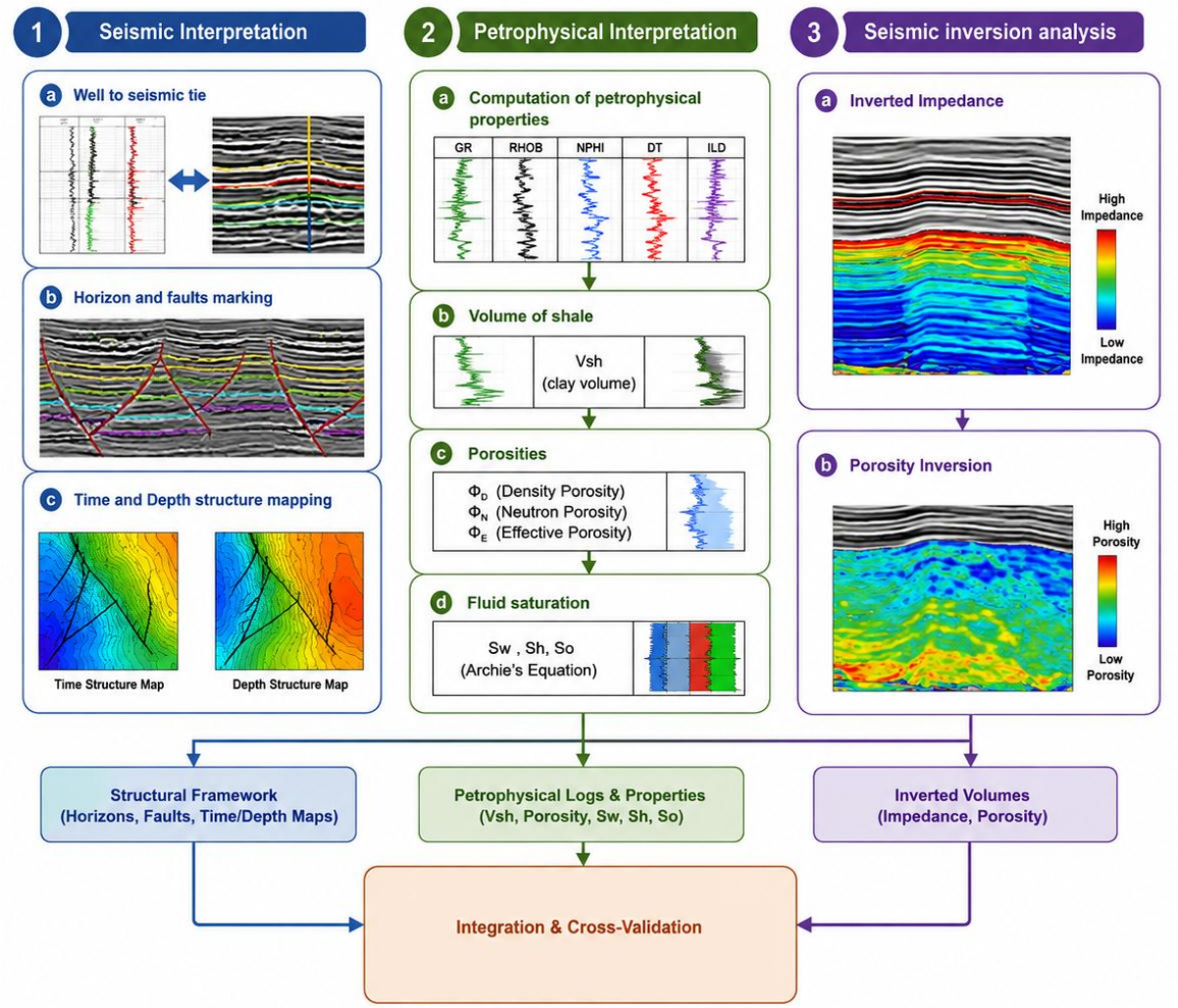

Fig. 4. Detailed step-by-step workflow adopted to conduct the research study.

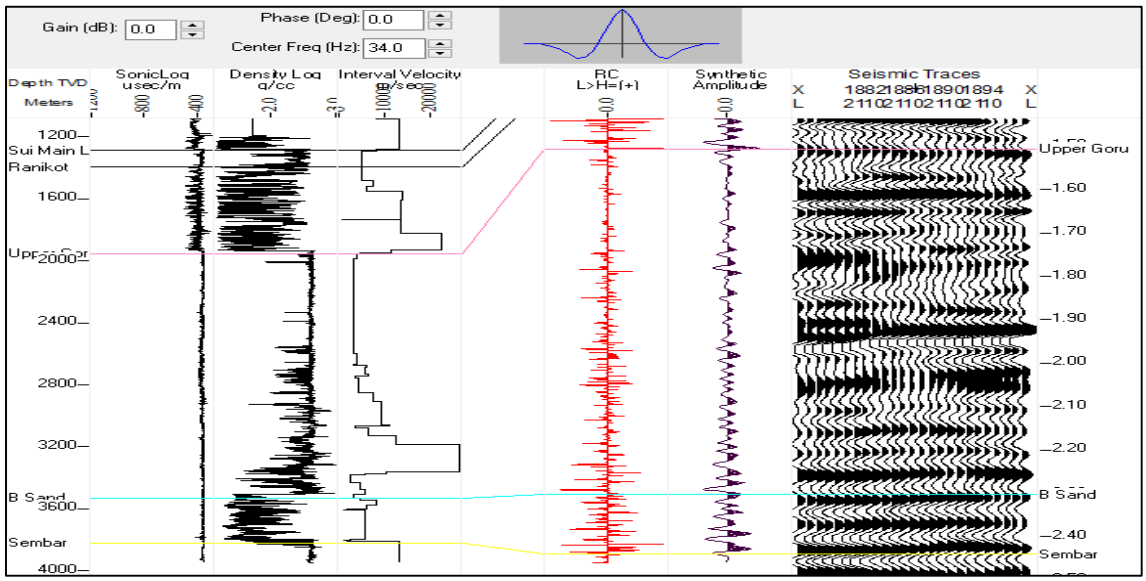

Fig. 5. Establishing well-to-seismic tie through synthetic seismogram of well Kadanwari-01.

Faults are marked on discontinuities, displacement, and breaks in reflectors. Better understanding of fault types in the area makes interpreters able to mark the continuation of seismic reflectors over a fault. It is important to identify the amount of vertical displacement of horizons along the faults. Time-domain seismic data is converted to the depth domain, which gives the possible depth of subsurface features. The accuracy of velocities gained from the check shot or vertical seismic profile surveys is essential to verify the accuracy of depth. These surveys provide Time vs Depth charts from which velocity can be obtained.

The interpreted fault segments on seismic profiles are correlated across the seismic cube by creating fault polygons to show definite structure. Horizons are marked on these time sections, which specify the beddings, i.e., lithological variations. TWT time maps are generated from these fault and horizon interpretations, which support delineating the structural geometry along with the fault orientation.

3.2 Petrophysics

The basic aim of petrophysics is to determine basic reservoir rock properties as well as quantitative measurements of reservoir fluids (Basit et al., 2025; Knackstedt et al., 2010). Wireline logs used in petrophysical analysis are effective tools utilized in the absence of core samples to estimate hydrocarbon presence, along with estimation of other vital rock attributes like porosity, permeability, lithology, pay and non-pay zones, etc. (Ali et al., 2019; Das and Chatterjee, 2018). Figure 6 shows a detailed step-by-step petrophysical analysis workflow for property computation using different log tracks and their application.

3.3 Seismic Inversion

Seismic inversion is the best tool for quantitative interpretation and provides a robust method to estimate the physical properties of rocks, especially the hydrocarbon-bearing strata. The Hampson-Russell (HRS) software is used for various kinds of seismic inversion (pre-stack and post-stack). The primary inputs to Hampson-Russell Software (HRS) for post-stack seismic inversion are the seismic volume and well data, which are used to generate an acoustic impedance volume. The convolution model, which underpins seismic inversion, allows for the creation of a synthetic trace, S (t), by convolution of the Earth's reflectivity series (RC) with a selected wavelet (Ahmed et al., 2023) such as:

$$S(t) = W(t) \times R + N \quad \ldots.(1)$$

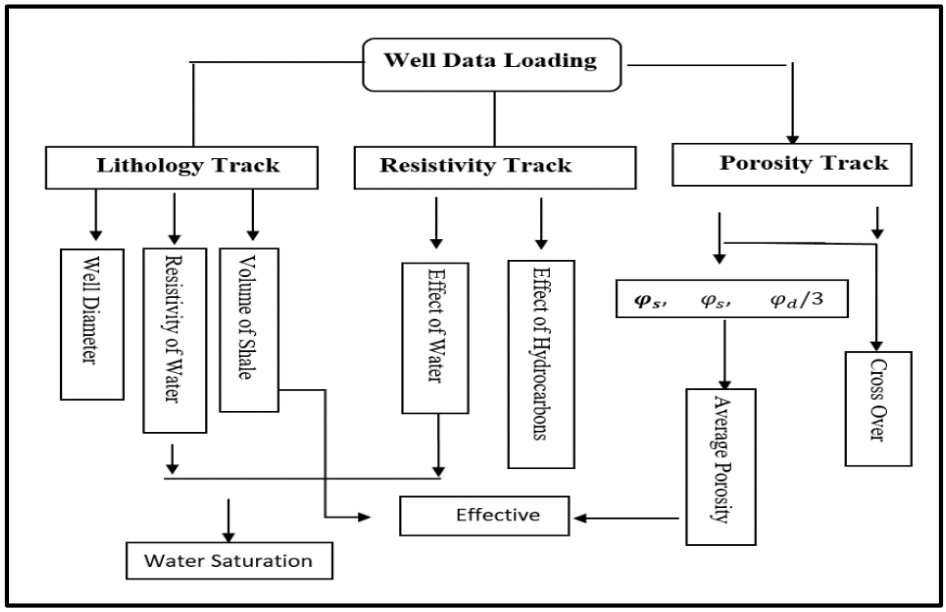

Fig. 6. Flow chart representation of petrophysical analysis (Ahmed et al., 2023).

Where R is the reflection coefficient (RC) series, W (t) represents the extracted statistical wavelet, and N represents the random noise. The steps involved in the seismic inversion process, illustrated in Figure 7, are discussed in detail in the following sections.

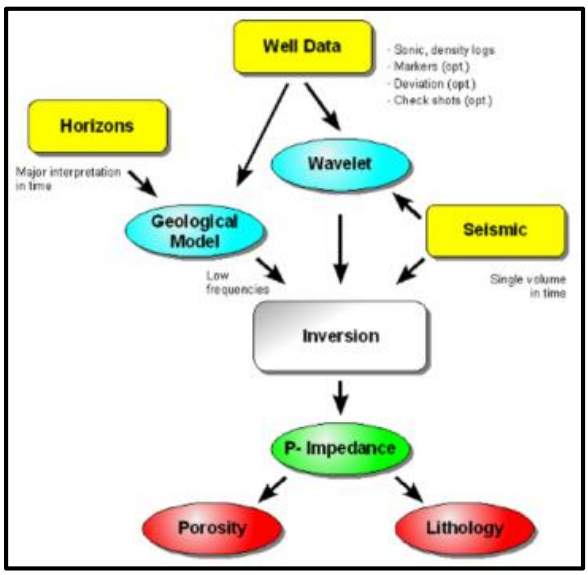

Fig. 7. Post-stack model-based inversion workflow showing required input data and output inverted attributes (Zhang et al., 2012).

3.3.1 Wavelet extraction and seismic to well tie

Both seismic data and all available well data are used in the wavelet extraction procedures. For building seismic inversion, the extracted wavelet needs to have a minimum phase or zero phase. The degree of phase shift in the extracted wavelet has a significant impact on the inversion results. If the phase shift is increased, there will be a high error in impedance (Shakir et al., 2022; Naseer et al., 2014).

Seismic inversion starts with the seismic-to-well correlation to get the best match between the two data sets. Wavelet is kept as zero phase and extracted first from the seismic data and then well base wavelet was utilized to get the maximum correlation and minimum error. Figure 8 shows the extracted wavelet having zero phase with 200 ms time. The time window is selected as one-fourth of the interpreted window. The extracted and inverted wavelet from the seismic data at the Kadanwari-01 well was projected using a constant zero-phase wavelet (Fig. 8). The window length for the extracted wavelet is selected from 1900ms to 2500ms and then extended to the whole volume.

3.3.2 Low Frequency (LF) Model

Seismic data contain the band-limited layer properties used for qualitative analysis; therefore, initial models or low-frequency models need relative AI for control. Absolute acoustic impedance is a property of an

absolute layer that is defined by model-based inversion and used for improved analysis (Shakir et al., 2024a). Absolute acoustic impedance can be estimated by incorporating an appropriate low-frequency model (typically 0–15 Hz) into the inversion process. Sparse-spike inversion provides relative impedance and is useful for qualitative seismic interpretation without requiring a separate low-frequency model (Shakir et al., 2024b). In this study, a low-frequency model was generated from the well-derived impedance curve over 1400–3000 ms, covering the B-Sand. The model restores the low-frequency components lost during seismic processing and stacking and provides an important input for model-based inversion. The frequency range used for the initial/low-frequency model ranges from 0–8 Hz.

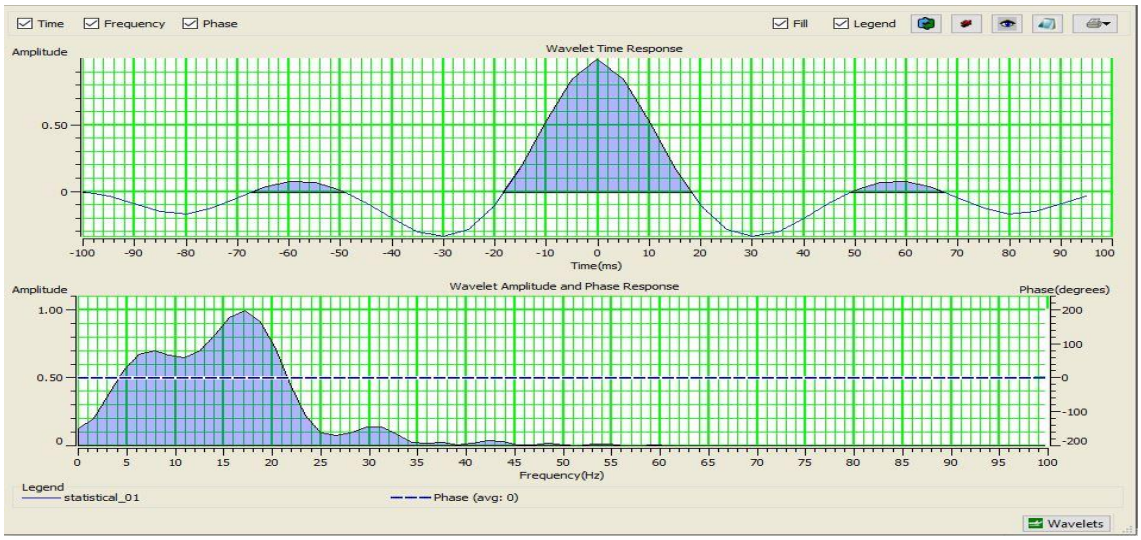

Fig. 8. Statistical wavelet extracted using seismic data input near well Kadanwari-01 in both time and frequency domains.

3.3.3 Model-Based Inversion

Statistical wavelet has been extracted from seismic data to refine the initial model using the universal linear inversion algorithm (Ahmed et al., 2023). Multiple iterations were run to get the best-fit match between the real and predicted data within an acceptable range. Until the discrepancy between the authentic seismic and predicted traces is eliminated, the geological model may be updated. The straightforward approach used in the inversion procedure is to account for any discrepancies between actual and predicted data (Shakir et al., 2022).

The model-based inversion was performed using Hampson-Russell software, with a 200 ms wavelet extracted from the seismic data. The principal inversion parameters included a sampling interval of 2 ms, 10 iterations, with 1% pre-whitening and a ±30% hard impedance constraint relative to the initial model. The inversion was constrained by the interpreted geological horizons and the well-derived impedance model. The quality of the inversion was assessed by comparing the synthetic seismic generated from the inverted impedance volume with the observed seismic data and by evaluating the agreement between the inverted impedance and the well-log-derived impedance at the calibration wells. The resulting acoustic impedance volume was subsequently used for porosity prediction through a porosity–impedance relationship.

3.3.4 Regression-Based Porosity Prediction

The spatial distribution of elastic parameter estimation is connected to the seismic data using regression-based porosity prediction analysis (i.e., petrophysical). For determining the relationship between various petrophysical parameters obtained from both seismic data and boreholes, regression methods are typically used. Linear regression is used to establish a statistical relationship between well-log data and seismic-derived properties. This relationship is then applied

across the available 3D seismic volume to estimate reservoir porosity. Following that, the calculated porosities are compared to those calculated inside the borehole to ensure accuracy (Ahmed et al., 2023; Hussain et al., 2023).

4 Results

4.1 Subsurface Structural Interpretation

To validate the structure in the subsurface, three horizons are interpreted, i.e., Upper Goru Formation, B-Sand, and Sembar Formation. Time and depth maps depict that all the marked horizons are deep on the eastern side while becoming shallow on the western side. Three normal faults, i.e., F1, F2, and F3, are interpreted at the B-Sand horizon level, and their orientation is evident in their respective maps. Extension and sliding developed these as listric faults in nature that divide the area into horst and graben. Fault F1 has NW-SE orientation and Fault F2 has NE-SW orientation forming graben structure whereas F3 has the same behavior as F2 as shown in B-Sand maps as shown in the Figure 9.

The depth contour interval is 20m whereas color bar shows the variations in the depth values in the map. Depth contours map of B-Sand ranges from 3,046-3,621 m shown in Figure 10. The contours are displayed on the map having unit in meters. An average velocity of about 3200m/s is used to convert time to depth for the targeted reservoir interval. Depth contours for B-Sand show relatively shallow depths in the western part of the study area, up to 3,046 m. The depth values show a consistent increase moving towards the eastern part, ranging up to 3,570 m.

4.2 Reservoir properties

In petrophysical analysis, reservoir zones are identified based on parameters like porosity (φ), volume of shale (V_{sh}), hydrocarbon saturation (S_h), water saturation (S_w), resistivity of water (R_w), etc., at Lower Goru B-Sand in Kadanwari-01, Kadanwari-03 and Kadanwari-10. After data quality analysis and extensive interpretation of well logs, pay intervals were marked in Kadanwari-01 and Kadanwari-10. Kadanwari-03 well showed good correlation based on the resistivity and porosity logs.

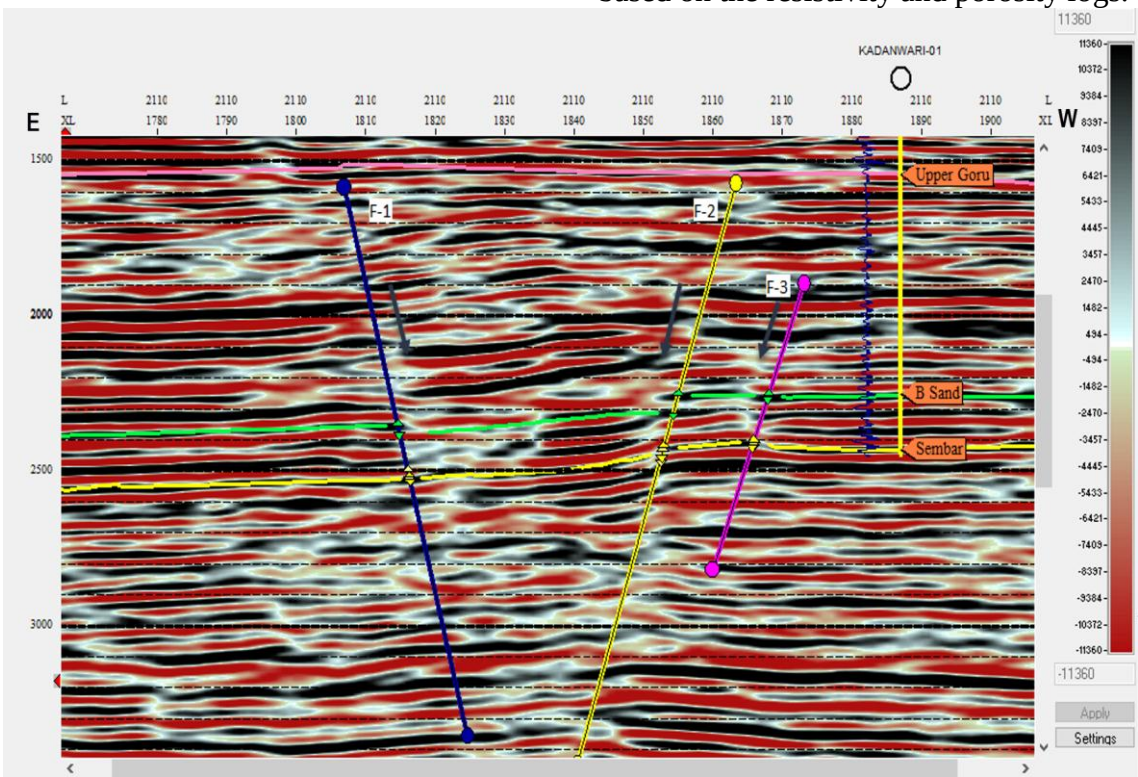

Fig. 9. Display of seismic inline 2110 showing the marked horizons and faults.

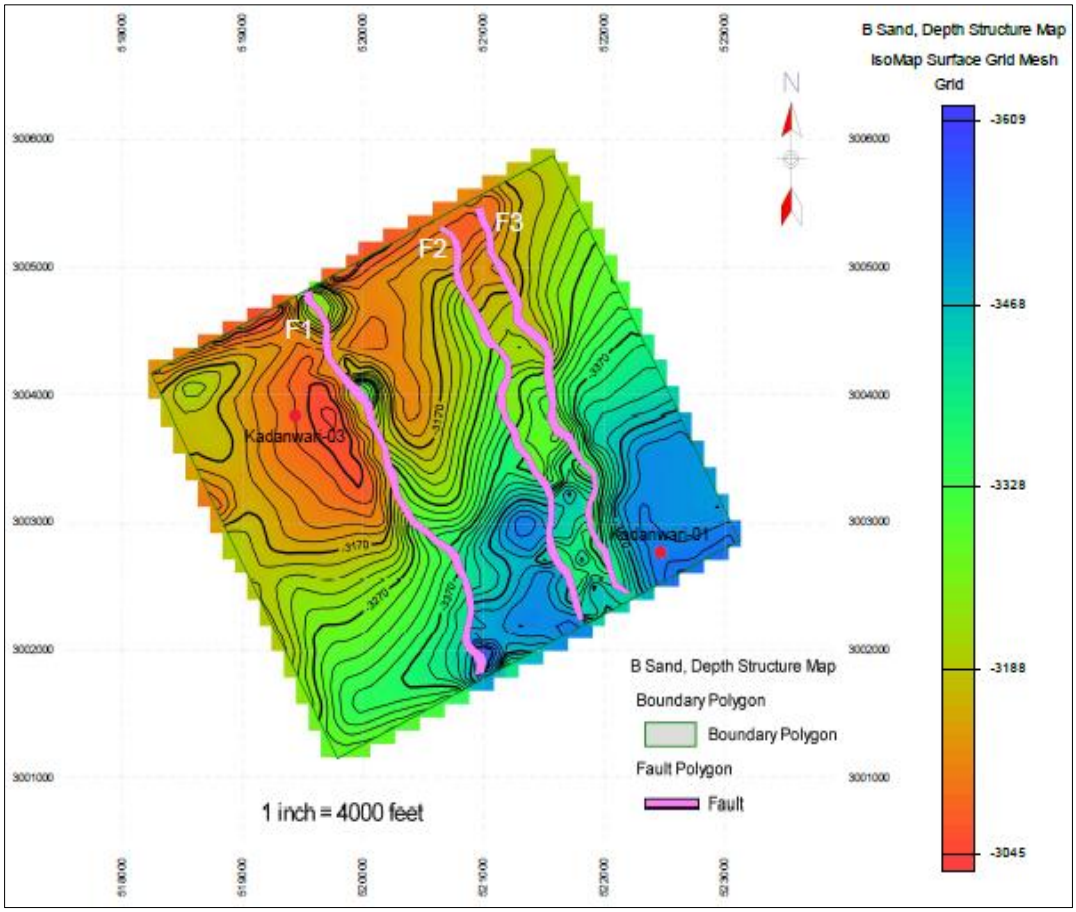

Fig. 10. Depth Contour map of B-Sand interval of LGF.

4.2.1 Petrophysical Analysis of Kadanwari-01

The results of the petrophysical analysis of Kadanwari-01 well show a potential zone of interest within B-Sand of the LGF ranging from 3506–3545 m (38.2m thick). It was marked as a potential zone because it has a low average volume of shale of about 10%, good effective porosity, i.e., almost 12%, and bears a high amount of hydrocarbon saturation, i.e., 58%, as evident in Figure 11.

4.2.2 Petrophysical Analysis of Kadanwari-03

In well Kadanwari-03, two zones of interest of 11.8 m and 30.0 m thickness were marked at the depth of 3322–3334 m and 3343–3373 m, respectively, in LGF (B-Sand) after Petrophysical analysis.

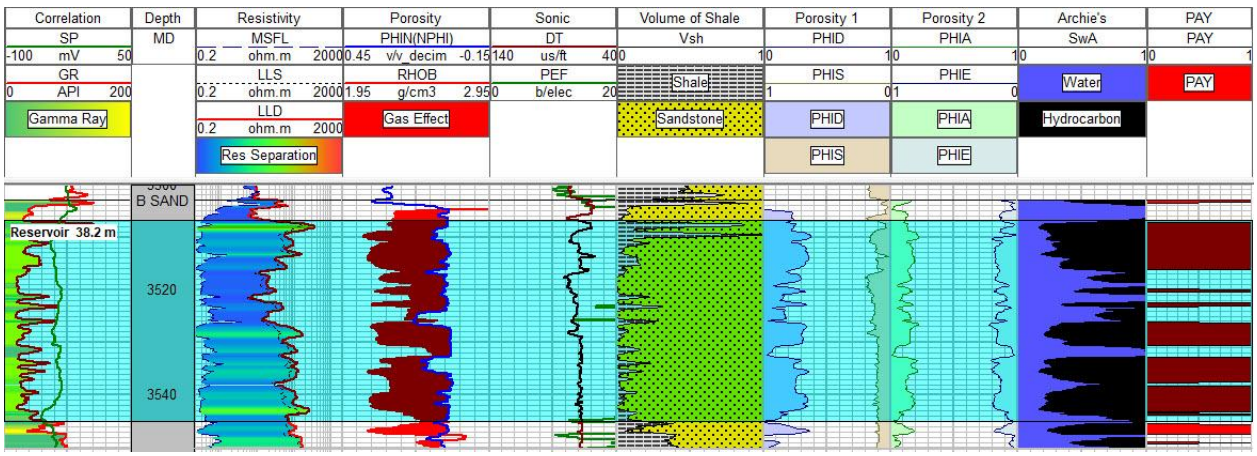

Fig. 11. Lower Goru B-Sand reservoir zone in Kadanwari-01 well with interpreted reservoir interval from 3506 – 3545 m.

Zone-01 has the average volume of shale about 29%, effective porosity almost 14% and hydrocarbon saturation 59 % whereas average volume of shale about 39%, effective porosity almost 10% and with hydrocarbon saturation 61% make zone-02 as a potential one as well (Fig. 12).

4.2.3 Petrophysical Analysis of Kadanwari-10

In Kadanwari-10, only one zone of 20.3 m thickness ranging from 3325 – 3346 m was marked as a hydrocarbon-bearing zone in LGF (B-sand) after Petrophysical analysis. Petrophysical interpretation shows 35% volume of shale, 10% effective porosity, and 63% hydrocarbon saturation in this potential zone (Fig. 13).

4.3 Inverted impedance

To develop a synthetic seismogram, the reflection coefficient computed from sonic and density logs at well Kadanwari-01 is convolved with an average well base wavelet extracted within a specific time window from seismic data. A good correlation between the synthetic seismogram and the seismic traces at the Kadanwari-01 well is observed, as shown in Figure 14. In correlation step seismic and well data is correlated with the synthetic trace which is generated by extracted wavelet. In seismic interpretation, correlation allows us to perform well-to-seismic tie. The maximum coefficient for correlation comes out to be 0.776 for the Kadanwari-01 well and related seismic data shown in (Fig. 14).

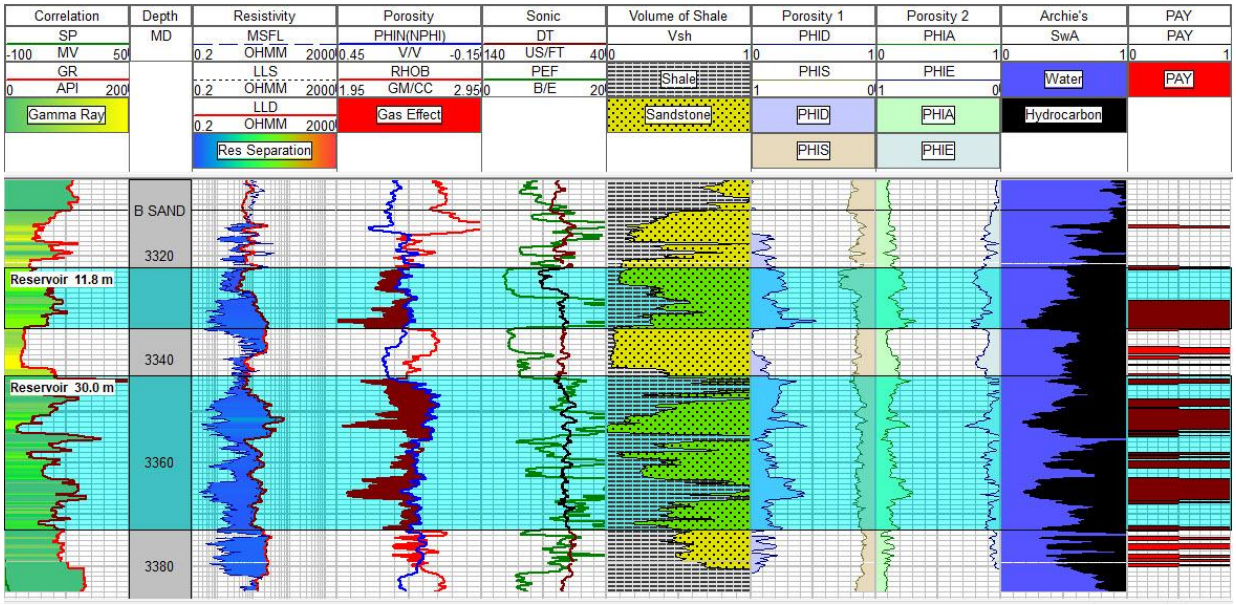

Fig. 12. Lower Goru B-Sand reservoir prospect zone in Kadanwari-03 well from 3322 – 3334 m and 3343 – 3373 m.

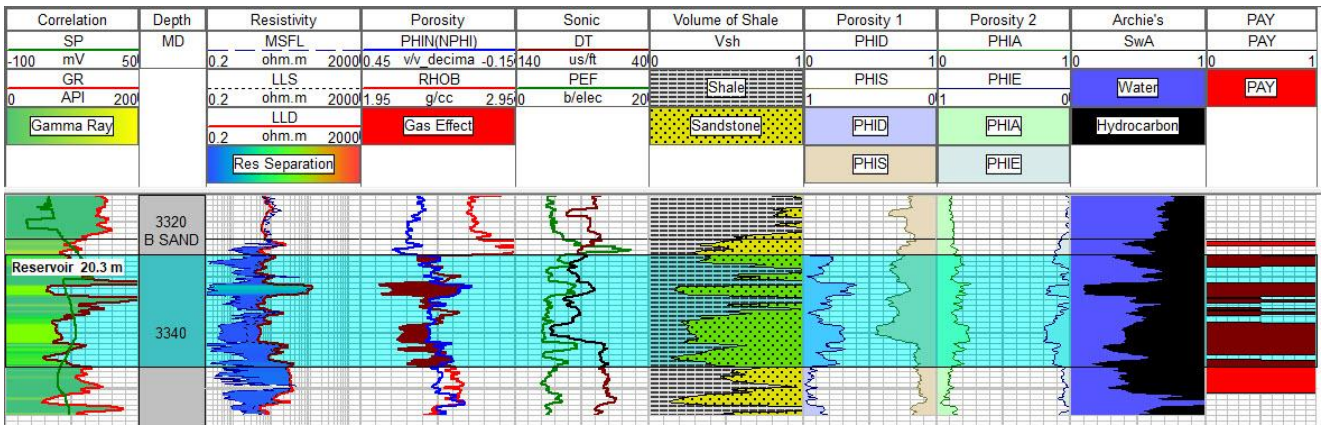

Fig. 13. Lower Goru B-Sand reservoir zone in Kadanwari-10 well from 3325 – 3346 m.

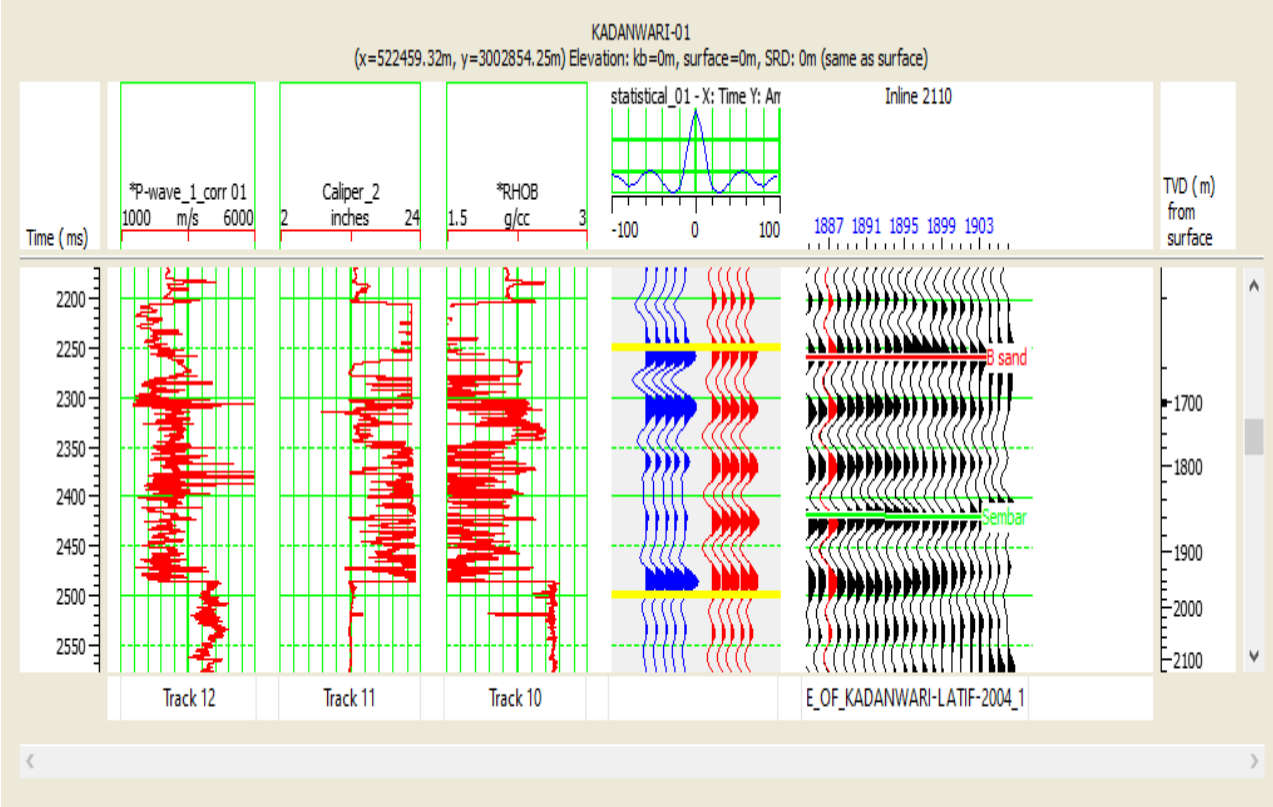

Fig. 14. Correlation of seismic and well data (Kadanwari-01) with synthetic trace.

Using the interpreted horizons and the missing low-frequency components (0–10 Hz) derived from the available well data, a low-frequency model (initial model) was generated (Fig. 15). A primary impedance model is made for the time range between 1900 and 2500 ms, which is where the targeted B-Sand interval is located, using the impedance curve produced by the well data. The low frequencies lost during stacking were retrieved via the initial model. For model-based inversion, this is a crucial variable. An iterative process is used to create a preliminary model before finding the model that best fits the synthetic trace and seismic data. The correlation is nearly 0.981, or 98.1%, after 20 adjustment iterations, with an error of 0.193, or 19.3%. This high percentage of correlation (Kadanwari-01) will lead to the generation of a reliable inverted impedance model (Fig. 16).

The entire final impedance model for the Kadanwari-01 well is displayed in Figure 17. The final inverted model is also overlaid with the impedance log generated from the well to demonstrate the well-to-seismic comparison. The main Kadanwari gas field production reservoir is the Lower Goru B-Sands. The final inverted impedance results shown at the targeted reservoir interval indicated low to moderate values throughout the interval, with high porosity values at the well location. The impedance slice at the B-sand interval of LGF is shown in Figure 18.

Since porosity depends on the lithology and fluid content of the formation, high porosity and low impedance can be related to defining the sweet spots at the desired reservoir level (Amjad et al., 2023). The zone of interest, B-sands of LGF at 2290 ms, has low impedance values ranging from 2801-3910 ((m/s)*(g/cc)), representing hydrocarbon presence. The high impedance contrast with yellow and red color shows this zone is gas-saturated. The high impedance layer (4649-6128 (m/s)*(g/cc)) present above this low impedance is believed to be act as a cap for B-sand reservoir with enhanced porosity on well location as porosity depend on lithology and fluid content in it. The observed low acoustic impedance is consistent with porous, gas-bearing sandstone, as supported by the corresponding petrophysical and well-log results.

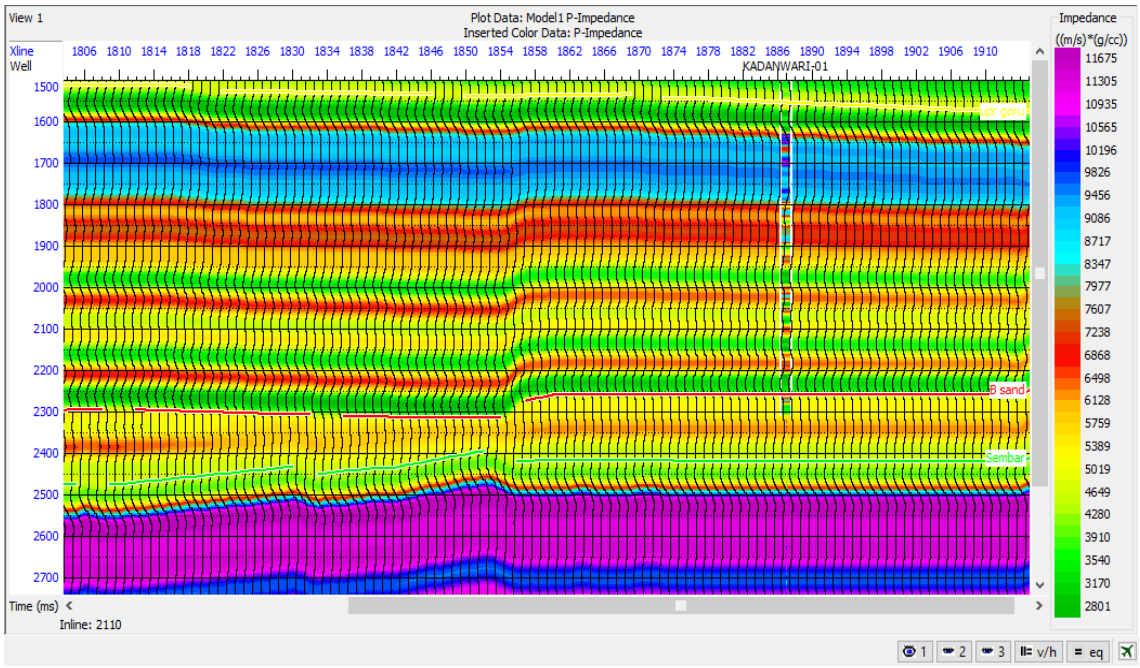

Fig. 15. Low-frequency model generated using the impedance curve of well Kadanwari-01.

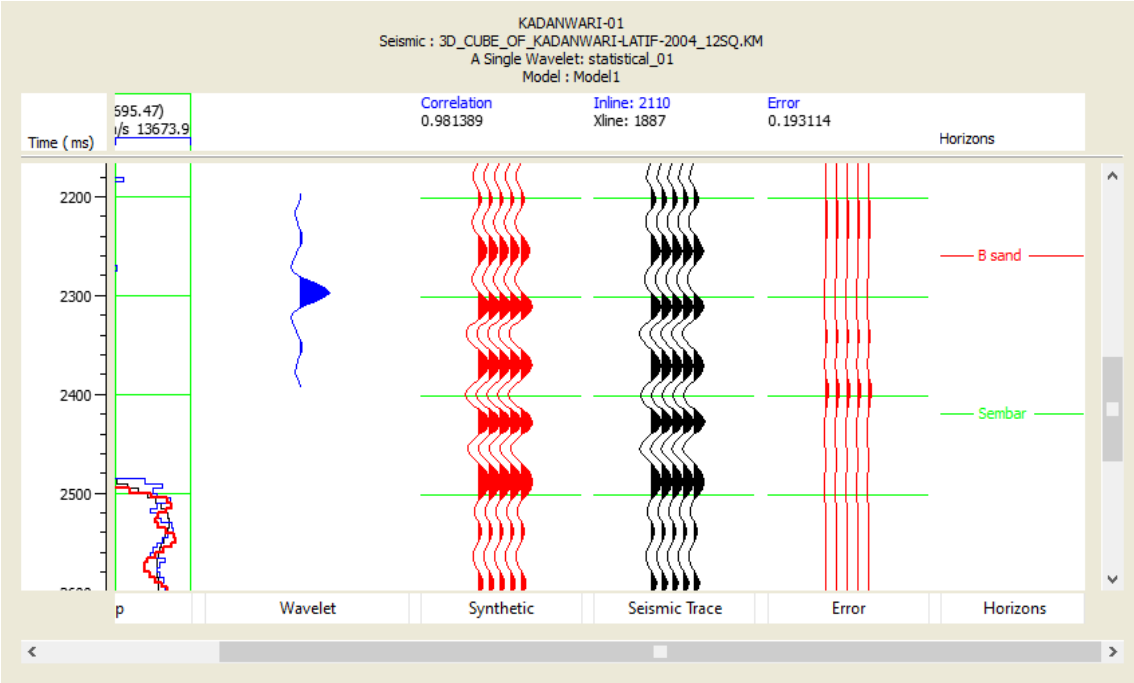

Fig. 16. Inversion analysis shows 98% correlation achieved after 20 iterations performed for the best-fit model between seismic data and synthetic trace.

4.3.1 Estimation of reservoir porosity

Porosity was statistically estimated after successfully inverting the seismic data. The inverted impedance was further used for the calculation of porosity here.

A relationship has been established (Eq. 2) using the regression analysis between the inverted impedances and actual porosities at the well location. A cross-plot method is used to correlate a porosity log from the well created during petrophysical analysis of the Kadanwari-01 well and an impedance log created during model-based inversion (Fig. 19). The correlation coefficient is reliable, which is calculated by using a linear regression. A linear relation with a negative slope is present between acoustic impedance and estimated porosity (Amjad et al., 2022). The linear relationship developed between

porosity and acoustic impedance by a best-fit regression line is given in Equation (2) as follows:

$$\varphi = -1.6041^{-5} \times A + 0.242382 \quad \ldots.(2)$$

Where φ represents the effective porosity, and a represents the inverted impedance from model-based inversion.

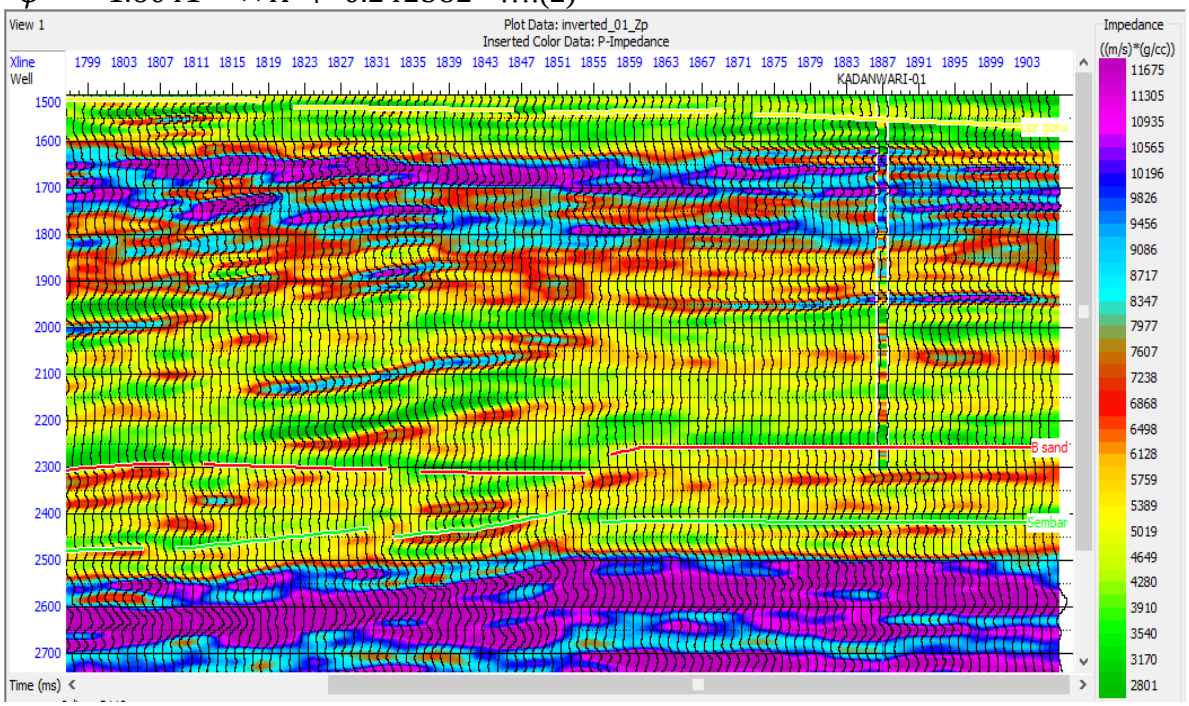

Fig. 17. Inverted impedance section at well Kadanwari-01.

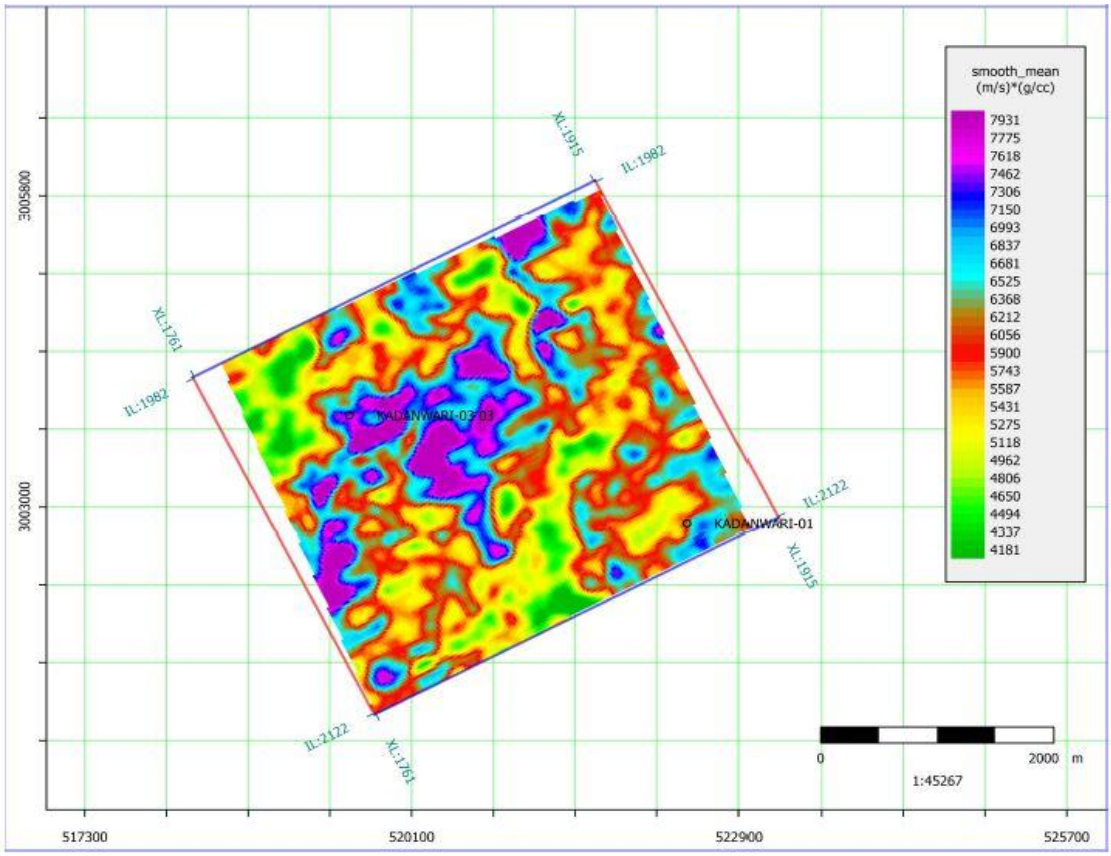

Fig. 18. Impedance slice of Kadanwari Block showing the impedance variation along the B-Sand.

For this analysis, a window of 100 ms below the targeted formation in the inverted section was selected. The log values for impedance, which lie within this window range, were plotted and correlated with the available porosity values in this zone. To get a maximum correlation, a best-fit line was passed through all plotted points to get the equation of the line for the whole zone. By using (Eq. 2), a good correlation with an 87% correlation coefficient (R^2) has been achieved for the plotted values, as shown in Figure 20.

5 Discussion

Accurate characterization of reservoirs is vital for effective drilling and minimizing uncertainty. Most of the discoveries in Pakistan are linked to the prolific Indus Basin. The exploration of thin gas sands deposited in heterogeneous environments like the LIB poses significant challenges due to reservoir heterogeneity and data limitations (Shakir et al., 2022). This study aimed to address these challenges via conventional seismic inversion methods along with conventional well log analysis.

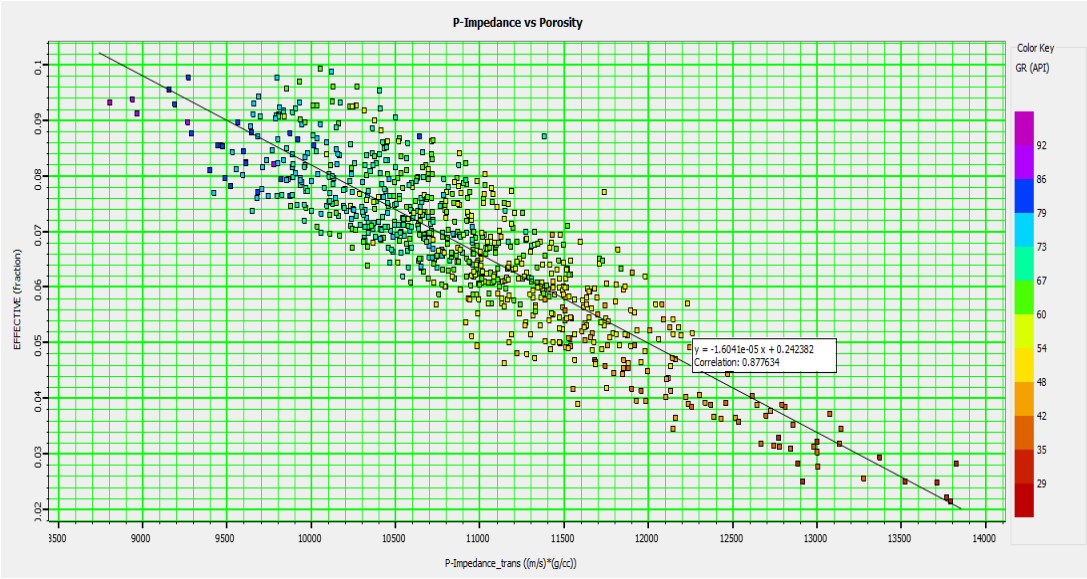

Fig. 19. Estimation of porosity using porosity log and impedance log of Kadanwari-01.

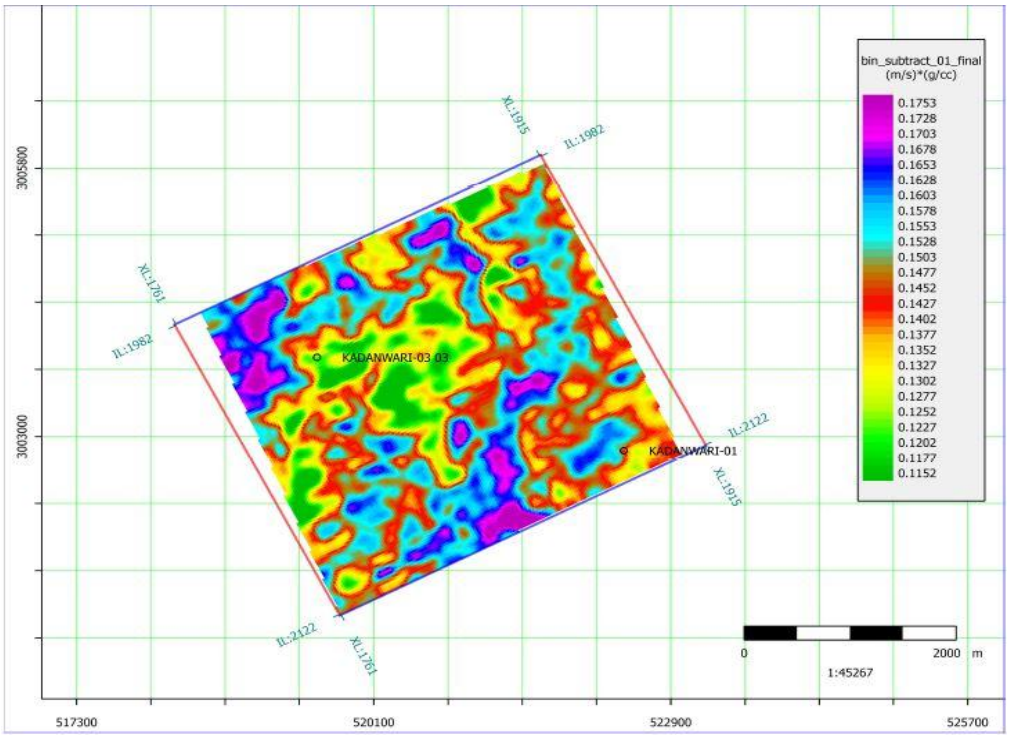

Fig. 20. Estimated porosity for B-interval sands in whole 3-D cube.

Lower Goru Formation is widely spread in the whole LIB and its equally important to have a complete trapping mechanism due to its variegated lithology of sand and shale. This depositional behavior makes this formation a promising target to be tapped. A lot of studies have been performed in many fields of LIB, like Sawan, Miano, and Gambat, producing from different sand intervals of the Lower Goru formations.

To understand the spatial lithological variations, reservoir properties, and to better understand the presence of potential zones, a seismic inverted impedance, along with seismic interpretation and petrophysical analysis on the Kadanwari-Latif block, has been carried out. Seismic interpretation has confirmed the presence of an extensional tectonic regime. Three faults, i.e., F1, F2, and F3, are interpreted in the B-Sand of the Lower Goru horizon on the seismic data as normal faults. The combination of extension with the sliding component causes listric faults that divide the area into horst and graben. The graben structure is formed by F1 and F2, two parallel normal faults, where the hanging wall is displaced downward, while the footwall is displaced in an upward direction. The faults, i.e., F1 and F2, are dipping toward the center of the graben from both sides, while F3 is a simple normal fault. The same assessments have been presented by Ali et al. (2019) and Ahmed et al. (2023). Petrophysical analysis of Kadanwari-01, 03 and 10 wells reveals the major reservoir zone at the B-Sand level and proves its potential as a hydrocarbon-bearing reservoir. These promising reservoir zones have shown a minimum of 58% hydrocarbon saturation in wells under study, i.e., Kadanwari-01, Kadanwari-03 and Kadanwari-10. These zones also showed good effective porosities.

Model-based seismic inversion methods have provided a better understanding of porosity and lithological content, especially of the B-Sand reservoir. The acoustic impedance contrast represented by color variations shows changes in lithological characteristics at different horizon levels. Results of the impedance model suggest low to moderate impedance values across the entire reservoir. In the producing zones, low values for impedance can be seen at the well location. Low values of impedance also support good porous zones (Ali et al., 2019). The porosity value ranges from 11% to 17% for the B-Sand calculated for the window of 100ms below the targeted horizon. An inverse relation exists between the porosity and inverted impedances here (Ehsan et al., 2018).

Porosity is always a critical element in reservoir characterization. This becomes very important to calculate between the wells, as the wells are located sparsely; seismic data play a vital role in these circumstances. If a good relationship has been developed between seismic elastic properties (inverted impedances) and porosities at well locations, then estimation away from the wells becomes possible. The primary objective of seismic inversion is not only to develop acoustic impedance models, but also to estimate other reservoir attributes such as clay volume, effective porosity, and hydrocarbon saturation for the spatial distribution away from well locations (Hussain et al., 2023).

The impedance distribution within the Lower Goru B-Sand reservoir predicts that the presence of low impedance values, along with the encouraging porosity distribution, marks the presence of potential zones. The statistically derived porosities range from 11% to 17% along this surface, which correlates with the petrophysically derived porosities. The validation of porosities at the well locations proves the authenticity of the results. To understand the variation and distribution of porosity and potential zones in the area, such techniques proved valuable for large-scale analysis over a whole 3D seismic volume.

6 Conclusions

The integration of conventional seismic interpretation along with seismic inversion and well analysis has given effective results for reservoir characterization. Reservoir characterization using petrophysical analysis has confirmed one hydrocarbon-bearing zone of significant

thickness and saturation in the B-Sand interval of LGF as a prospect reservoir in the Kadanwari area. The presence of horst and graben structure confirmed by seismic interpretation which were further validated by contour maps. Seismic inversion has revealed the low-impedance layer bounded by high impedance. The model-based inversion efficiently stated lithological variations along with low impedance ranging from 6800-7900 (m/s*g/cc) within the reservoir zone in high resolution. Spatial distribution of estimated porosity based on inversion within the B-Sand ranges from 11% to 17%. This analysis indicated porosity values ranging from 10% to 14%, which fairly match the average values of the porosities computed in all three wells using wireline log data. The adopted methodology can be usefully applied in similar basins having identical structural settings to characterize potential reservoirs.

Authors' Contribution

Urooj Shakir proposed the main concept and was involved in the write-up and proofreading of the manuscript. Muhammad Raiees Amjad provided relevant literature, assisted in the preparation of figures, and conducted a technical review before submission. Muyyassar Hussain assisted in establishing seismic inversion analysis and porosity estimation. Muhammad Haris Siddiqui collected data and performed the petrophysical analysis.

Acknowledgments

The authors express their gratitude to the Department of Earth Sciences, University of Haripur, and Department of Earth and Environmental Sciences at Bahria University Islamabad for their assistance and support throughout this research study. The authors would also like to express their sincere thanks to GeoSoftware and LMK Resources for the provision of geoscience interpretation software Hampson Russell and GVERSE GeoGraphix, respectively. The authors also extend their sincere gratitude to the Directorate General of Petroleum Concession for permitting public domain data for research study.

Data Availability

Data sets used in this study are available from the authors upon reasonable request.

Conflict of interest

The authors assert that the study has been conducted without any commercial or financial affiliations that may be interpreted as a possible source of conflict of interest.

References

Abubakar, M., Qadir, A., Amjad, M. R., Rehman, Q. U., Zahid, M., & Taimur, A. (2026). Stratigraphic architecture and reservoir quality variability assessment of Cretaceous deltaic deposits of Lower Goru Formation using well log data. *Journal of Sedimentary Environments*, *11*(4). https://doi.org/10.1007/s43217-026-00330-4

Ahmad, N., & Chaudhry, S. (2002). Kadanwari gas field, Pakistan: A disappointment turns into an attractive development opportunity. *Petroleum Geoscience*, *8*(4), 307–316. https://doi.org/10.1144/petgeo.8.4.307.

Ahmad, N., Fink, P., Sturrock, S., Mahmood, T., & Ibrahim, M. (2004). Sequence stratigraphy as predictive tool in Lower Goru Fairway, Lower and Middle Indus platform, Pakistan. Proceedings of the SPE-PAPG Annual Technical Conference, 85–104.

Ahmad, N., Spadini, G., Palekar, A., & Subhani, M. A. (2007). Porosity prediction using 3D seismic inversion: Kadanwari gas field, Pakistan. *Pakistan Journal of Hydrocarbon Research*, *17*, 95–102.

Ahmad, S., & Ghazi, S. (2022). Depositional trends and reservoir geometries of the Early Cretaceous Lower Goru Formation in Lower Indus Basin, Pakistan: Evidence from sequence stratigraphy. *Journal of Petroleum Exploration and Production Technology*, *12*, 2981–3001. https://doi.org/10.1007/s13202-022-01489-y.

Ahmad, S., Ahmad, F., Ullah, A., Eisa, M., Ullah, F., Kaif, K., & Khan, S. (2019). Integration of the outcrop and subsurface geochemical data: Implications for the hydrocarbon source rock evaluation in the Lower Indus Basin, Pakistan. *Journal of Petroleum Exploration and Production Technology*, *9*, 937–951. https://doi.org/10.1007/s13202-018-0569-6.

Ahmed, S. A., Hussain, M., & Khan, Z. U. (2023). The application of the PNN algorithm to evaluate the petrophysical properties of the heterogeneous E-sand reservoirs, Lower Goru Formation, Pakistan. *Kuwait Journal of Science*, *50*(4), 773–782. https://doi.org/10.1016/j.kjs.2023.02.032.

Ahmed S.A., MonaLisa, Hussain M., & Khan Z. U. (2022) Supervised machine learning for predicting shear sonic log (DTS) and volumes of petrophysical and elastic attributes, Kadanwari Gas Field, Pakistan. *Frontiers in Earth Science*. 10:919130. doi: 10.3389/feart.2022.919130

Ali, A., Alves, T. M., Saad, F. A., Ullah, M., Toqeer, M., & Hussain, M. (2018). Resource potential of gas reservoirs in South Pakistan and adjacent Indian subcontinent revealed by post-stack inversion techniques. *Journal of Natural Gas Science and Engineering*, *49*, 41–55. https://doi.org/10.1016/j.jngse.2017.10.010

Ali, A., Zubair, H. M., Hussain, M., Rehman, K., & Toqeer, M. (2016). Effect of shale distribution on hydrocarbon sands integrated with anisotropic rock physics for AVA modelling: A case study. *Acta Geophysica*, *64*(4), 1139–1163. https://doi.org/10.1515/acgeo-2016-0041

Ali, M., Khan, M. J., Ali, M., & Iftikhar, S. (2019). Petrophysical analysis of well logs for reservoir evaluation: A case study of Kadanwari gas field, Middle Indus Basin, Pakistan. *Arabian Journal of Geosciences*, *12*, Article 215. https://doi.org/10.1007/s12517-019-4389-x.

Ali, N., Chen, J., Fu, X., Hussain, W., Ali, M., Hussain, M., & Thanh, H. V. (2022). Prediction of Cretaceous reservoir zone through petrophysical modeling: Insights from Kadanwari gas field, Middle Indus Basin. *Geosystems and Geoenvironment*, *1*(3), Article 100058. https://doi.org/10.1016/j.geogeo.2022.100058.

Ali, S. K., Janjuhah, H. T., Shahzad, S. M., Kontakiotis, G., Saleem, M. H., Khan, U., Zarkogiannis, S. D., Makri, P., & Antonarakou, A. (2021). Depositional sedimentary facies, stratigraphic control, paleoecological constraints, and paleogeographic reconstruction of Late Permian Chhidru Formation (Western Salt Range, Pakistan). *Journal of Marine Science and Engineering*, *9*(12), Article 1372. https://doi.org/10.3390/jmse9121372.

Amjad, M. R., Khan, S., Nisar, U. B., Shakir, U., & Ahmed, K. A. (2022). Exploring the untapped gas potential of Ghazij shale in Pirkoh area, Pakistan: Integrated approach of attribute analysis and maturity modeling. *Turkish Journal of Earth Sciences*, *31*(1), 1–19. https://doi.org/10.3906/yer-2105-36

Amjad, M. R., Zafar, M., Malik, M. B., & Naseer, Z. (2023). Precise geopressure predictions in active foreland basins: An application of deep feedforward neural networks. *Journal of Asian Earth Sciences*, *245*, Article 105560. https://doi.org/10.1016/j.jseaes.2023.105560.

Babasafari, A. A., Ghosh, D. P., Salim, A. M., & Kordi, M. (2020). Integrating petroelastic modeling, stochastic seismic inversion, and Bayesian probability classification to reduce uncertainty of hydrocarbon prediction: Example from Malay Basin. *Interpretation*, *8*(3), SM65–SM82. https://doi.org/10.1190/INT-2019-0077.1

Bachrach, R., Sengupta, M., Salama, A., & Miller, P. (2009). Reconstruction of the layer anisotropic elastic parameters and high-resolution fracture characterization from P-wave data: A case study using seismic inversion and Bayesian rock physics parameter estimation. *Geophysical Prospecting*, *57*(2), 253–262. https://doi.org/10.1111/j.1365-2478.2008.00768.x.

Basit, A., Qadir, A., Amjad, M. R., Ahmad, T., & Khattak, S. A. (2025). Petroleum reservoir potential of Cretaceous siliciclastic rocks of Tando Allahyar Field, Lower Indus Basin,

Pakistan: Inferences from petrophysics, sequence stratigraphy and paleogeography. *Doklady Earth Sciences*, *520*, 1–15. https://doi.org/10.1134/S1028334X24604097.

Craig, J., Hakhoo, N., Bhat, G. M., Hafiz, M., Khan, M. R., Misra, R., Pandita, S. K., Raina, B. K., Thurow, J., Thusu, B., Ahmed, W., & Khullar, S. (2018). Petroleum systems and hydrocarbon potential of the North-West Himalaya of India and Pakistan. *Earth-Science Reviews*, *187*, 109–185. https://doi.org/10.1016/j.earscirev.2018.09.012

Dar, Q. U. Z., Renhai, P., Ghazi, S., Ahmed, S., Ali, R. I., & Mehmood, M. (2023). Depositional facies and reservoir characteristics of the Early Cretaceous Lower Goru Formation, Lower Indus Basin Pakistan: Integration of petrographic and gamma-ray log analysis. *Petroleum*, *9*(3), 331–341. https://doi.org/10.1016/j.petlm.2021.09.003

Das, B., & Chatterjee, R. (2018). Well log data analysis for lithology and fluid identification in Krishna-Godavari Basin, India. *Arabian Journal of Geosciences*, *11*(10), Article 231. https://doi.org/10.1007/s12517-018-3587-2.

Dobrin, M. B., & Savit, C. H. (1988). *Introduction to geophysical prospecting (4th ed.)*. McGraw-Hill.

Ehsan, M., Gu, H., Akhtar, M. M., Abbasi, S. S., & Ehsan, U. (2018). A geological study of reservoir formations and exploratory well depths statistical analysis in Sindh Province, Southern Lower Indus Basin, Pakistan. *Kuwait Journal of Science*, *45*(2), 84–93. https://journals.ku.edu.kw/kjs/index.php/KJS/article/view/3290

Hampson, D., Todorov, T., & Russell, B. (2000). Using multi-attribute transforms to predict log properties from seismic data. *Exploration Geophysics*, *31*(3), 481–487. https://doi.org/10.1071/EG00481.

Hussain, M., Khan, Z. U., & Ahmed, S. A. (2023). Quantifying thin heterogeneous gas sand facies of Rehmat gas field by developing petro elastic relationship in fine stratigraphic layers through Bayesian stochastic seismic inversion. *Marine and Petroleum Geology*, *149*, Article 106074. https://doi.org/10.1016/j.marpetgeo.2022.106074.

Kearey, P., Brooks, M., & Hill, I. (2002). *An introduction to geophysical exploration (3rd ed.)*. Blackwell Science.

Khalid, P., Farid, A., Naseer, M. T., Yasin, Q., & Naseem, S. (2023). Seismic stratigraphy and attributes application for imaging a Lower Cretaceous deltaic system: Sukkur rift zone, Lower Indus Basin, Pakistan. *Marine and Petroleum Geology*, *149*, 106030. https://doi.org/10.1016/j.marpetgeo.2022.106030

Khan, M. J., & Khan, H. A. (2018). Petrophysical logs contribute in appraising productive sands of Lower Goru Formation, Kadanwari concession, Pakistan. *Journal of Petroleum Exploration and Production Technology*, *8*, 1089–1098. https://doi.org/10.1007/s13202-018-0472-1.

Khan, Z. U., MonaLisa, Hussain, M., & Ahmed, S. A. (2023). Bayesian stochastic inversion with petro-elastic relation to quantify thin gas sands of Khadro Formation, Zamzama gas field. *Episodes*, *46*(3), 389–405. https://doi.org/10.18814/epiiugs/2022/022039

Knackstedt, M., Jaime, P., Butcher, A. R., Botha, P. W., Middleton, J., & Sok, R. (2010). Integrating reservoir characterization: 3D dynamic, petrophysical and geological description of reservoir facies. In *SPE Asia Pacific Oil and Gas Conference and Exhibition*. SPE. https://doi.org/10.2118/133981-MS

Ma, X. Q. (2002). Simultaneous inversion of prestack seismic data for rock properties using a global simulated annealing. *Geophysics*, *67*(6), 1877–1885. https://doi.org/10.1190/1.1527087.

Mukerji, T., Jørstad, A., Avseth, P., Mavko, G., & Granli, J. R. (2001). Mapping lithofacies and pore-fluid probabilities in a North Sea reservoir: Seismic inversions and statistical rock physics. *Geophysics*, *66*(4), 988–1001. https://doi.org/10.1190/1.1487078.

Naeem, M., Jafri, M. K., Moustafa, S. S. R., Al-Arifi, N. S., Asim, S., Khan, F., & Ahmed, N. (2016). Seismic and well log driven structural and petrophysical analysis of the Lower

Goru Formation in the Lower Indus Basin, Pakistan. *Geosciences Journal*, *20*(1), 57–75. https://doi.org/10.1007/s12303-015-0028-z

Nanda, N. C. (2016). Seismic data interpretation and evaluation for hydrocarbon exploration and production: A practitioner's guide. Springer. https://doi.org/10.1007/978-3-319-26491-2.

Naseer, T. M., Asim, S., Ahmad, M. N., Hussain, F., & Qureshi, S. N. (2014). Application of seismic attributes for delineation of channel geometries and analysis of various aspects in terms of lithological and structural perspectives of Lower Goru Formation, Pakistan. *International Journal of Geosciences*, *5*(12), 1490–1502. https://doi.org/10.4236/ijg.2014.512121.

Rashid, M., Luo, M., Ashraf, U., Hussain, W., Ali, N., Rahman, N., Hussain, S., Martyushev, D. A., Thanh, H. V., & Anees, A. (2022). Reservoir quality prediction of gas-bearing carbonate sediments in the Qadirpur field: Insights from advanced machine learning approaches of SOM and cluster analysis. *Minerals*, *13*(1), Article 29. https://doi.org/10.3390/min13010029.

Shakir, U., Ali, A., Hussain, M., Azeem, T., & Bashir, L. (2022). Selection of sensitive post-stack and pre-stack seismic inversion attributes for improved characterization of thin gas-bearing sands. *Pure and Applied Geophysics*, *179*(1), 169–196. https://doi.org/10.1007/s00024-021-02900-1

Shakir, U., Ali, A., Hussain, M., Radwan, A. E., & El Aal, A. A. (2024a). PNN enhanced seismic inversion for porosity modeling and delineating the potential heterogeneous gas sands via comparative inversion analysis in the Lower Indus Basin. *Pure and Applied Geophysics*, *181*, 2801–2821. https://doi.org/10.1007/s00024-024-03562-5.

Shakir, U., Ali, A., Hussain, M., Radwan, A. E., El Aal, A. A., Amjad, M. R., & Mahmood, M. F. (2024b). Data-driven exploration in complex basins: A critical aspect of new prospect delineation in thin sands using simultaneous seismic inversion. *Journal of Earth System Science*, *133*(4), Article 229. https://doi.org/10.1007/s12040-024-02438-5.

Sohail, G. M., Hawkes, C. D., & Yasin, Q. (2020). An integrated petrophysical and geomechanical characterization of Sembar Shale in the Lower Indus Basin, Pakistan, using well logs and seismic data. *Journal of Natural Gas Science and Engineering*, *78*, Article 103327. https://doi.org/10.1016/j.jngse.2020.103327.

Tiab, D., & Donaldson, E. C. (2015). Petrophysics: Theory and practice of measuring reservoir rock and fluid transport properties (4th ed.). Gulf Professional Publishing

Umar, M., Friis, H., Khan, A. S., Kassi, A. M., & Kasi, A. K. (2011). The effects of diagenesis on the reservoir characters in sandstones of the Late Cretaceous Pab Formation, Kirthar Fold Belt, southern Pakistan. *Journal of Asian Earth Sciences*, *40*(2), 622–635. https://doi.org/10.1016/j.jseaes.2010.10.014.

Zhang, R., Sen, M. K., Phan, S., & Srinivasan, S. (2012). Stochastic and deterministic seismic inversion methods for thin-bed resolution. *Journal of Geophysics and Engineering*, *9*(5), 611–618. https://doi.org/10.1088/1742-2132/9/5/611.